CHEMICAL ENGINEERING TRANSACTIONS
VOL. 86, 2021
A publication of AIDIC
The Italian Association of Chemical Engineering
Online at www.cetjournal.it
Guest Editors: Sauro Pierucci, Jiří Jaromír Klemeš

ISBN 978-88-95608-84-6; **ISSN** 2283-9216
DOI: 10.3303/CET2186137

Photocatalytic Activity of Visible-light-driven Ternary Ag/Ag_2S/ZnO Nanocomposites for Phenol Degradation in Water

Emmanuel O. Ichipi*, Shepherd M. Tichapondwa, Evans M. N. Chirwa

Water Utilisation and Environmental Engineering Division, Department of Chemical Engineering, University of Pretoria, Pretoria 0002.
emmanuel.ichipi91@gmail.com

Silver sulphide (Ag_2S) and zinc oxide (ZnO) nanoparticles were synthesized through a sol-gel method. The Ag constituent of the ternary was achieved by photodesposition of the binary Ag_2S/ZnO resulting in a color change from brownish grey to purple indicating its formation. The synthesised particles were characterised using Scanning electron microscopy (SEM), Transmission electron microscopy (TEM) and Energy-dispersive X-ray spectroscopy (EDX) to confirm its elemental presence and morphology. The crystallinity of the nanoparticles was determined using the X-ray diffractometer (XRD), and Brunauer–Emmett–Teller (BET) analysis surface area was 4.95 m^2g^{-1}. The progressive degradation of phenol was analysed and results showed that under visible light, the ternary composite Ag/Ag_2S/ZnO, exhibited the highest phenol degradation efficiency (95 %) compared to the constituent compounds, ZnO (37 %) and Ag2S/ZnO (83 %) after 6 h of visible light irradiation respectively. However, investigations have revealed that extrinsic factors such as pH of the solution, the initial concentration of phenol and photocatalyst dosage could significantly affect the overall system performance.

1. Introduction

Nearly 3.2 million children die annually in developing countries owing to the consumption of polluted water and living in unhygienic environments (Raizada et al., 2019). The UN World Water Development has reported that approximately 750 million persons are not privileged to consume clean water and the need for water for industrial purposes will rise by 400 % before 2050 (Chan et al., 2011). The evolution of industrial development and technology in modern times has led to the continuous release of toxic substances to the ecosystem which are lethal to the health of humankind. Phenolic compounds, a priority organic pollutant present in water due to discharges or natural phenomenon are known to be highly toxic and can pose a serious threat to the ecosystem even at low concentrations (Villegas et al., 2016). They can be carcinogenic to vital organs of the human body and can cause unpleasant taste and odour to water (Anku et al., 2017). The earlier traditional wastewater treatment techniques such as coagulation and flocculation, membrane separation, natural aerobic treatment, precipitation, and Fenton process are subjected to various limitations. These include low sustainability, high operational costs, chemical instability, high sludge generation, separation difficulties and long processing time (Hofman-Caris and Hofman, 2017). Although microbial breakdown using pure/mixed cultures might be a much more friendly process, it has not proven to be as effective as advanced oxidation processes (AOPs) (Vincenzo Naddeo, 2013). AOPs are generally known for their high efficiency to degrade a wide range of organic pollutants at reasonably low cost, as it is able to convert renewable solar energy into a chemical reaction. This is done by utilizing the ability of the hydroxyl and superoxide anions radicals that are generated by a series of chemical reactions in the oxidation process to degrade aqueous contaminants into less harmful products (Raizada et al., 2019). Semiconductor based heterogeneous photocatalysis is one efficient AOPs that utilizes solar or visible light irradiation to degrade recalcitrant organic pollutants into their mineral constituents. The traditional use of ultraviolet (UV) irradiation which constitutes only about 4% of the entire solar radiation that reaches the earth's surface is not techno-economically feasible especially for a

Paper Received: 2 November 2020; Revised: 20 February 2021; Accepted: 2 May 2021
Please cite this article as: Ichipi E., Tichapondwa S., Chirwa E.M., 2021, Photocatalytic Activity of Visible-light-driven Ternary Ag/Ag_2S/ZnO Nanocomposites for Phenol Degradation in Water, Chemical Engineering Transactions, 86, 817-822 DOI:10.3303/CET2186137

large-scale water treatment process. With the balance of the spectrum being 43 % visible and 53 % infrared lights, many attempts have been made to develop visible light active photocatalysts (Samadi et al., 2016). The unique properties of metal oxides nanoparticles play a vital part in chemistry, physics and material science applications because most catalysts consist of oxide as active phase (Zheng, 2009).

In the last two decades, Zinc oxide (ZnO) has been widely studied as an alternative to TiO_2 in the photocatalytic degradation of various pollutants owing to its wide direct band gap (3.4 eV) high photosensitivity in the solar spectrum, optical properties, low cost, chemical stability, and environmental friendliness (Abdelhakim et al., 2015). However, some limitations restricts its application such as fast electron/hole recombination rates, particle aggregation, and activation under UV light only (Iqbal et al., 2014). This can be improved by modifying ZnO with transition metallic cations and non-metallic anions resulting in a reduction in the electron/hole recombination rate and increased visible light responsiveness (Lavand and Malghe, 2016). Under visible light irradiation, Fe and C doping on ZnO nanoparticles showed better photo-absorption capacity than pure ZnO. Although Fe exhibited a much higher performance than C because of the Fe^{3+} cations that acted as shallow holes in the lattice of the catalyst (Lavand and Malghe, 2016). Similarly, the addition of metal halides and sulfides, such as AgCl, AgBr, CdS, and Ag_2S, via coupling effect can significantly improve the photocatalytic performance of semiconductor oxides (Chen et al., 2016). A binary nanocomposite was developed by doping ZnO using Silver Sulphide (Ag_2S) whose band gap is much narrower (1.1 eV) to red shift its light sensitivity from 400 nm to the visible light region. Considering the optical properties of Ag_2S, two reactions proceeded; the binary without light absorption (dark) to isolate oxidation-reduction and further irradiation for Ag^+ ions reduction to form a ternary Ag/Ag_2S:ZnO (Kryukov et al., 2004). The second reaction has shown more adsorption efficiency corresponding to the attributes of Surface Plasmon Resonance (SPR) absorption bands of silver-based nanomaterials. In this study, a ternary $Ag/Ag_2S/ZnO$ nanocomposite was synthesised using a hydrothermal method and characterised using various techniques. The main purpose of this work is to develop a method for increasing the photosensitivity of ZnO nanoparticles in the visible light region to investigate the degradation of phenol in water.

2. Experimental

2.1 Chemicals and reagents

Zinc acetate dehydrate ($Zn(CH_3COO)_2.2H_2O$) and sodium hydroxide (NaOH) were used as precursors for the formation of ZnO. Silver nitrate ($AgNO_3$) and sodium sulphide (Na_2S) were the reactants for Ag_2S and distilled water was used throughout. All the chemical reagents and other solvents for this study were used as obtained from the suppliers without any purification.

2.2 Synthesis

Pure ZnO and Ag_2S/ZnO nanocomposites were prepared via a hydrothermal technique and $Ag/Ag_2S/ZnO$ by photodesposition method. 2.23 g of $Zn(CH_3COO)_2.2H_2O$ was dissolved in 25 ml of 0.2 M NaOH and 25 ml distilled water to form a transparent solution of the desired concentration. The mixture was placed in stainless steel autoclave (with Teflon inner liner) at 120 °C for 2 h, the white precipitate formed was then separated by centrifugation. The supernatant was removed, and the precipitate (ZnO precursor) was washed 3 times each with distilled water and ethanol before drying in an oven. The ZnO precursor was subjected to calcination in a furnace at 900 °C for 3 h to remove all the volatile substances to form pure ZnO which was then ground into powder. The binary nanocomposite Ag_2S/ZnO was prepared by dissolving 0.5 g of pure ZnO in a 50ml solution of 60/40 % v/v methanol and distilled water. 0.08 g of $AgNO_3$ was added to the solution and sonicated for 40 min to agitate the particle mixture. Finally, 0.03 g of Na_2S was added with continuous stirring for 8 h in the dark to avoid surface plasmon resonance of the Ag constituent. The resultant precipitate was obtained using filter papers, placed in an oven 70 °C for 12 h to dry up and then ground to powder. The ternary $Ag/Ag_2S/ZnO$ nanocomposite was prepared by re-dispersing a suitable amount of Ag_2S/ZnO in distilled water with constant stirring under visible light for 4 h. A change in color was observed indicating oxidation-reduction of the Ag^+ cations has occurred. The solution was again centrifugated at 9000 rpm for 15 min, kept in an oven at 70 °C for 12 h to dry and ground with a mortar into powder before it was used. The underlying chemical reactions that occurred during the synthesis of the ZnO are summarized as follows:

$$Zn(CH_3COO)_2.2H_2O + 2NaOH \rightarrow Zn(OH)_2 + 2CH_3COONa + 2H_2O \quad (1)$$

$$Zn(OH)_2 + 2H_2O \leftrightarrow Zn^{2+} + 2OH^- + 2H_2O \leftrightarrow [Zn(OH)_4]^{2-} \quad (2)$$

$$[Zn(OH)_4]^{2-} \leftrightarrow ZnO_2^{-2} + 2H_2O \quad (3)$$

$$ZnO_2^{-2} + 2H_2O \leftrightarrow ZnO + 2OH^- \quad (4)$$

2.3 Characterisation of catalysts

The SEM images and EDS analysis were done on a Zeiss Ultra PLUS FEG SEM and the TEM pictures on a JOEL JEM 2100F TEM. The XRD analysis was done using an X-ray radiated from a Fe filtered Co-Kα radiation (wavelength, ʎ =1.789 Å). The crystallography of the materials was obtained by choosing the best–matching standards from the ICSD database, using X'Pert Highscore plus software. BET analysis to determine the specific surface area of the particles was carried out on a Micrometrics Tristar II with liquid nitrogen temperature of 77.350 K.

2.4 Degradation analytical method

The progressive degradation of phenol concentration was analysed using a High-Performance Liquid Chromatography (HPLC – waters 2695 separation module, 2996 Photodiode Array detector) with a Waters PAH C-18 (5µm, 4.6 x 250 mm, 2 – 8 pH range) spherical column, and monitored with an Empower software. The parameters for detection of phenol are column temperature at 35 °C (±5), injection volume of 10 µL, a flow rate of 1.0 $mLmin^{-1}$, a wavelength of 280 nm, and a mobile phase of 0.1 % of acetic acid in acetonitrile and water at 50 % each. Standards of phenol concentration at 2-10 ppm were used to calibrate the method and the retention time for each sample was 6 min overall but phenol was detected at 3.50 min. The total degradation of phenol after 6 h was evaluated with the following expression.

$$\% \text{ Degradation} = \frac{(C_0 - C_t)}{C_0} \times 100 \quad (5)$$

Such that C_0 (mgL^{-1}) is the initial phenol concentration and C_t (mgL^{-1}) is the concentration of phenol at any given time, t.

3. Results and discussions

3.1 XRD pattern

The X-ray diffraction patterns of the prepared ZnO, Ag_2S/ZnO and Ag/Ag_2S/ZnO nanoparticles are shown in Figure 1. The peaks are intense and narrower at (100), (002), (101), (102), (110), (103) and (112) planes which indicates the high purity of hexagonal wurtzite crystalline structure of the ZnO materials (Amornpitoksuk et al., 2012). The highest intensity of the (101) peak is an indication of the anisotropic growth and preference of the crystallites. For confirmation purposes, the diffraction peaks of the synthesized ZnO and Ag_2S/ZnO matched well compared with the standard XRD patterns of ZnO (JCPSD 36-1451). There was no impurity phase detected which means that the Zn^{2+} can be substituted by Ag^+ without changing its solid state. The high peaks can be assigned to the wurtzite phase of ZnO. The modification of ZnO with Ag_2S did not affect its crystallinity overall, however, a small peak is noticed at about 45° that can be attributed to the presence of Ag^+ in the nanocomposite.

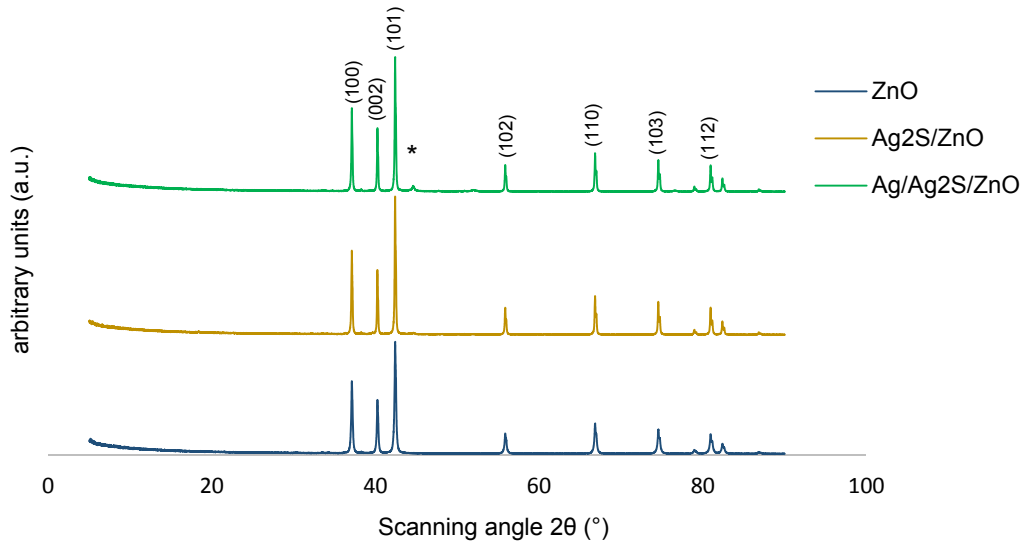

Figure 1: XRD pattern of crystalline ZnO, Ag_2S/ZnO and Ag/Ag_2S/ZnO

3.2 SEM, TEM and EDX analysis

The morphologies and structures of the synthesised pure ZnO nanoparticles, after it was modified with Ag_2S and further photodesposition into a ternary Ag/Ag_2S/ZnO is shown in Figure 2(a-c). It shows that the doping of Ag_2S on the surface of ZnO was done without destroying or changing its morphology which is a very influential factor in its photocatalytic activity. The SEM images reveal a mix of highly porous spherical sheets and nanorods with wide particle size distribution however, it must be noted that the method of synthesis determines the structural and morphological properties of the material. The TEM images shown in Figure 2(d-f) confirm perfect spherical and hexagonal rod like structures detected in the SEM analysis with diameters and lengths between 25 to 40 nm and 200 to 400 nm, respectively. It is observed that the addition of Ag_2S into the ZnO matrix decreased the growth of microrods.

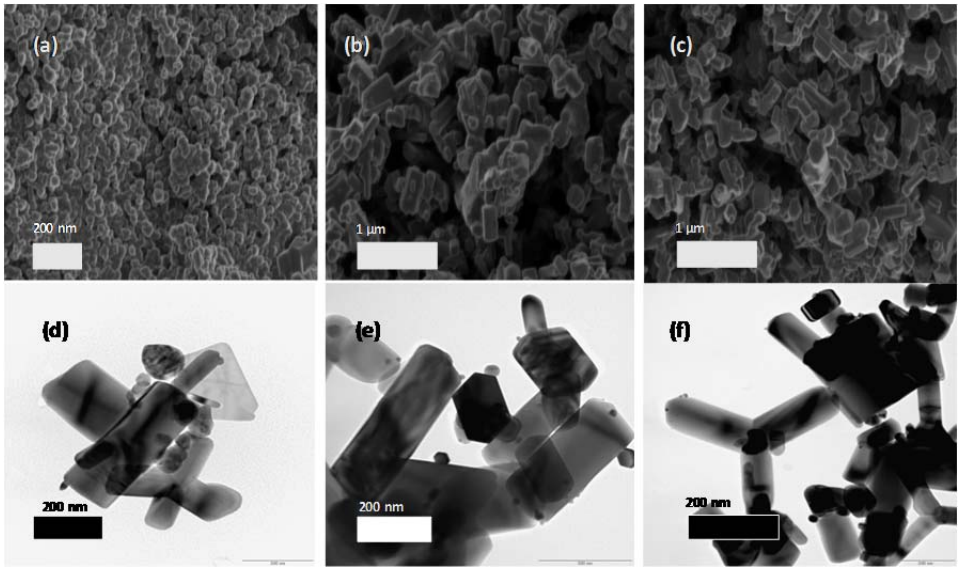

Figure 2: SEM (a), (b), (c) and TEM (d), (e), (f) images of ZnO, Ag_2S/ZnO and Ag/Ag_2S/ZnO

The EDX analysis detected the amount of all the constituent compounds Zn, Ag, S and O in the ternary catalyst as 71.1 wt%, 18.4 wt%, 0.1 wt% and 6.4 wt% respectively as shown in Figure 3. The remaining percentage consisted of sodium and carbon which were identified as trace elements in the nanopowder.

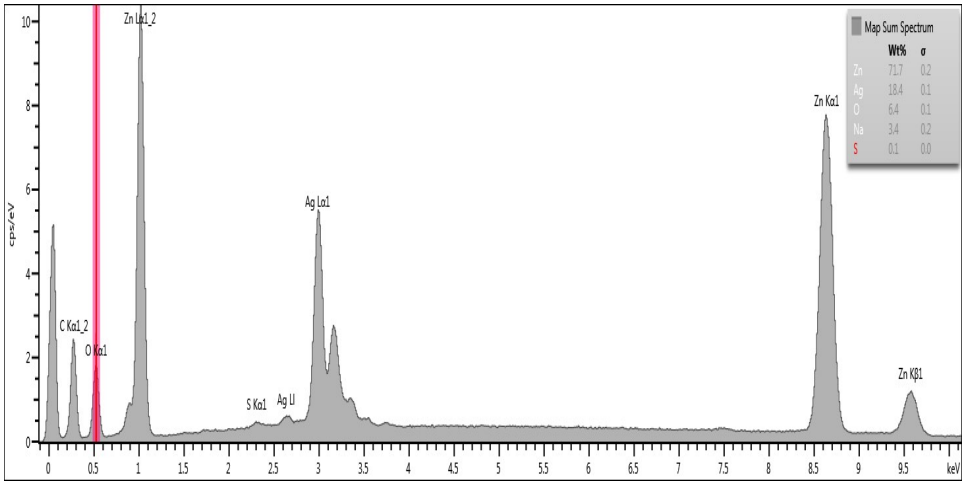

Figure 3: EDX spectra of ternary Ag/Ag_2S/ZnO nanopowder.

3.3 BET surface area

The specific surface area (S_{BET}) and pore size distribution of all three nanopowders were measured by N_2 adsorption-desorption isotherms. Table 1, reveals a minor shrinkage in the surface area of ZnO to Ag_2S/ZnO from 4.95 to 4.62 m^2g^{-1} and BJH adsorption average pore width from 59.77 to 56.79 Å. This reduction may be due to the effect of Ag_2S coating which resulted into collapse of the pores and particles agglomeration. However, further photodesposition of the binary regained the surface area but still reduced the BJH adsorption and desorption average pore width.

Table 1: Surface area and pore size measurement of sorbents by BET analysis

Materials	Surface Area (m^2g^{-1})	BJH Adsorption * (4V/Å)	BJH Desorption * (4V/ Å)
ZnO	4.95	59.77 Å	60.57 Å
Ag_2S/ZnO	4.62	56.79 Å	60.28 Å
Ag/Ag_2S/ZnO	4.95	54.44 Å	55.42 A

**Average pore width*

3.4 Photocatalytic Study

The photodegradation of the prepared catalysts was studied on the decontamination of phenol in water in the presence of visible light. The experiments were performed on 10 mg/L phenol concentration at a 100 ml volume using 0.8 g/L of catalyst loading. The experimental setup was a box consisting of stirrers and three 18 W fluorescent day light lamps for the visible light simulation. An adsorption test was first performed for 30 min in the dark so the reaction can get to an adsorption-desorption balance. Figure 4 reveals a photolysis test (light only) carried on the pollutant that had 5 % degradation and an adsorption test (no light) with the ternary catalyst that recorded 14 % degradation. Although some contaminants can be degraded by direct photolysis, but the most commonly used radiation has wavelenght in the range of 200–400 nm (UV spectrum region). Likewise, in adsorption, when saturation is reached at the surface of the active sites available in the nanoparticle, the adsorption bond can be broken, thereby releasing the adsorbent from adsorbate which then results to regeneration of the pollutants by the desorption. The as-synthesised ZnO catalyst had a 37 % degradation in 6 h which is lesser compared to its 98 % degradation of ortho- nitrophenol in 5 h under UV light as reported by Assi et al. (2014). The modified ternary Ag/Ag_2S/ZnO nanocomposite exhibited the highest degradation efficiency at 95 % than Ag_2S/ZnO which had 83 % degradation in 6 h. The SPR and dipolar effect of Ag^+ ions attract visible light which increases absorption and photodegradation, however, excess deposition on the surface may lead to light blocking and reduced photocatalytic activity (Jiao et al., 2018).

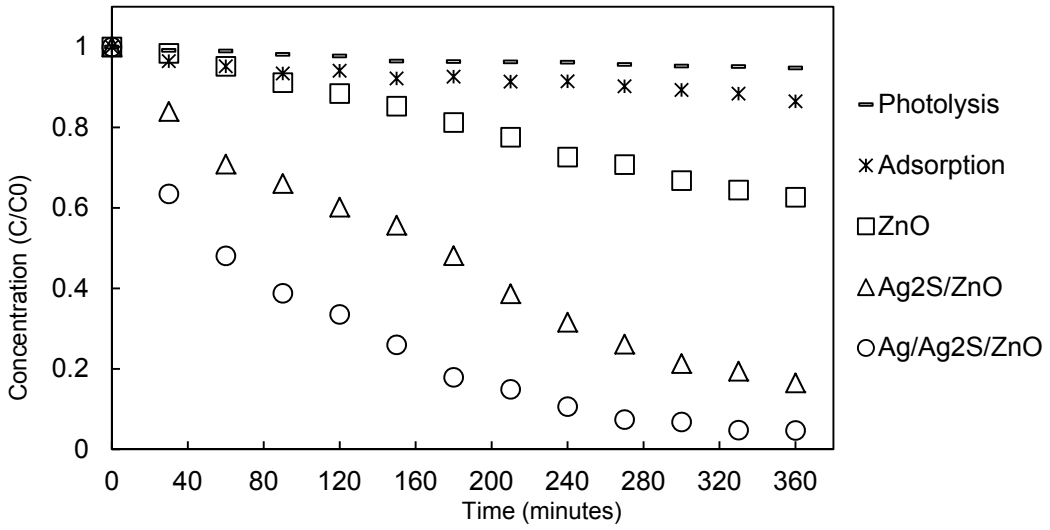

Figure 4: Phenol degradation with time under visible light irradiation

4. Conclusions

In this paper, the photoactivity of ZnO doped with Ag_2S nanoparticles which were prepared by hydrothermal process, was investigated in the degradation of phenol in water under visible light. The physical and chemical properties of the nanocomposites have been revealed using XRD, SEM, TEM, EDX and BET characterisation studies. Results proved that the interaction between the ZnO and Ag_2S did not only improve the transfer of charges and recombination rate of the photogenerated electron-hole pairs but also broadened its absorption spectrum into the visible light region. The Ag_2S acted as a catalyst for metallic Ag^+ ions reduction with the visible light conforming with the absorption band of the binary Ag_2S/ZnO.

References

Abdelhakim Z., Meftah A., Jaber A., Abdelaziz A. A., Aida M. S., 2015, Annealing Effects on the Structural, Electrical and Optical Properties of ZnO Thin Films Prepared by Thermal Evaporation Technique, *Journal of King Saud University - Science,* 426.

Amornpitoksuk P., Suwanboon S., Sangkanu S., Sukhoom A., Muensit N., Baltrusaitis J., 2012, Synthesis, Characterization, Photocatalytic and Antibacterial Activities of Ag-Doped ZnO Powders Modified with a Diblock Copolymer, *Powder Technology,* 219**,** 158-164.

Anku W. W., Mamo M. A., Govender P. P., 2017, Phenolic Compounds in Water: Sources, Reactivity, Toxicity and Treatment Methods.

Assi N., Mohammadi A., Sadr Manuchehri Q., Walker R., 2014, Synthesis and Characterization of ZnO Nanoparticle Synthesized by a Microwave-Assisted Combustion Method and Catalytic Activity for the Removal of Ortho-Nitrophenol. *Desalination and Water Treatment***,** 1-10.

Chan S., Wu T., Juan J. C., Teh C., 2011, Recent Developments of Metal Oxide Semiconductors as Photocatalysts in Advanced Oxidation Processes (AOPs) for Treatment of Dye Wastewater. *Journal of Chemical Technology and Biotechnology,* 86**,** 1130-1158.

Chen C., Li Z., Lin H., Wang G., Liao J., Li M., Lv S., Li W., 2016, Enhanced Visible Light Photocatalytic Performance of ZnO Nanowires Integrated with Cds and Ag2s. *Dalton Transactions,* 45**,** 3750-3758.

Hofman-Caris R., Hofman J., 2017, Limitations of Conventional Drinking Water Technologies in Pollutant Removal.

Iqbal J., Jan T., Ronghai Y., Naqvi M. S. H., Ahmad I., 2014, Doping Induced Tailoring in the Morphology, Band-Gap and Ferromagnetic Properties of Biocompatible ZnO Nanowires, Nanorods and Nanoparticles. *Nano Letters,* 6**,** 242-251.

Jiao Z., Zhang J., Liu Z., Ma Z., 2018, Ag/Agcl/Ag2moo4 Composites for Visible-Light-Driven Photocatalysis. *Journal of Photochemistry and Photobiology A: Chemistry,* 371.

Kryukov A. I., Stroyuk O., Zin'chuk N. N., Korzhak A. V., Kuchmii S. Y., 2004, Optical and Catalytic Properties of Ag2S Nanoparticles. *Journal of Molecular Catalysis A: Chemical,* 221**,** 209–221.

Lavand A., Malghe Y., 2016, Synthesis, Characterization and Visible Light Photocatalytic Activity of Carbon and Iron Modified ZnO. *Journal of King Saud University - Science,* 30.

Raizada P., Sudhaik A., Singh P., 2019, Photocatalytic Water Decontamination using Graphene and ZnO Coupled Photocatalysts: A Review. *Materials Science for Energy Technologies,* 2**,** 509-525.

Samadi M., Zirak M., Naseri A., Khorashadizade E., Moshfegh A. Z., 2016, Recent Progress on Doped ZnO Nanostructures for Visible-Light Photocatalysis. *Thin Solid Films,* 605**,** 2-19.

Villegas L., Mashhadi N., Chen M., Mukherjee D., Taylor K., Biswas N., 2016, A Short Review of Techniques for Phenol Removal from Wastewater. *Current Pollution Reports,* 2.

Vincenzo Naddeo A. C., 2013, Wastewater Treatment by Combination of Advanced Oxidation Processes and Conventional Biological Systems. *Journal of Bioremediation & Biodegradation,* 04.

Zheng Z., 2009, Synthesis and Modifications of Metal Oxide Nanostructures and their Applications.